Journal of Molecular Structure 1200 (2020) 127174

Contents lists available at ScienceDirect

Journal of Molecular Structure

journal homepage: http://www.elsevier.com/locate/molstruc

Syntheses of N-substituted benzimidazolone derivatives: DFT calculations, Hirshfeld surface analysis, molecular docking studies and antibacterial activities

Asmaa Saber [a], Nada Kheira Sebbar [a, b, **], Yusuf Sert [c, *], Nabil Alzaqri [d], Tuncer Hökelek [e], Lhoussaine El Ghayati [a], Ahmed Talbaoui [f], Joel T. Mague [g], Yassir Filali Baba [h], Martine Urrutigoîty [i], El Mokhtar Essassi [a]

[a] Laboratoire de Chimie Organique Hétérocyclique, Centre de Recherche des Sciences des Médicaments, Pôle de Compétences Pharmacochimie, Mohammed V University in Rabat, Faculté des Sciences, Av. Ibn Battouta, BP 1014, Rabat, Morocco
[b] Laboratoire de Chimie Appliquée et Environnement, Equipe de Chimie Bioorganique Appliquée, Faculté des Sciences, Université Ibn Zohr, Agadir, Morocco
[c] Bozok University, Department of Physics, Yozgat, Turkey
[d] Department of Chemistry, King Saud University, P.O. Box 2455, Riyadh, 11451, Saudi Arabia
[e] Department of Physics, Hacettepe University, 06800, Beytepe, Ankara, Turkey
[f] Laboratoire de Biologie des Pathologies Humaines, Faculté des Sciences, Université Mohammed V, Rabat, Morocco
[g] Department of Chemistry, Tulane University, New Orleans, LA, 70118, USA
[h] Laboratoire de Chimie Organique Appliquée, Université Sidi Mohamed Ben Abdallah, Faculté des Sciences et Techniques, BP 2202, Fez, Morocco
[i] Laboratory of Coordination Chemistry, LCC, University of Toulouse, CNRS, Toulouse, France

ARTICLE INFO

Article history:
Received 24 July 2019
Received in revised form
28 September 2019
Accepted 1 October 2019
Available online 2 October 2019

Keywords:
Benzimidazolone
Crystal structure
Hirshfeld surface
Molecular docking
DFT
Antibacterial activity

ABSTRACT

New benzimidazolone derivatives (**2**–**5**) were synthesized and characterized using NMR and single crystal X-ray diffraction techniques. Along with the experimental data, the predicted spectral data were also obtained using density functional theory (DFT) at the B3LYP/6-31G(d,p) level of theory. In addition, the closest contacts between the active atoms of the compounds were identified through Hirshfeld surface analyses, molecular docking studies, and DFT calculations. The antibacterial activities of derivatives (**2**–**5**) against gram-positive and gram-negative microbial strains, such as *Staphylococcus aureus*, *Escherichia coli*, and *Pseudomonas aeruginosa* were also evaluated, and the results obtained showed the antibacterial activities of derivatives (**2**–**5**) using a minimum inhibitory concentration (MIC) assay.

1. Introduction

In recent years, heterocyclic compounds have received considerable attention due to their significant importance in pharmacological and agricultural fields [1–7]. Notably, nitrogen heterocyclic compounds are known to exhibit excellent biological and pharmaceutical activities [3–5]. In fact, benzimidazole derivatives have been extensively studied in different areas of chemistry, including pharmaceutical and other chemical industries [5–7]. The benzimidazole core has several active sites and provides a great responsiveness, making it an excellent heterocyclic precursor in the syntheses of new heterocyclic compounds. With respect to the biological applications of benzimidazolone derivatives, these derivatives are found to possess potent antioxidant [8], antiparasitic [9], anthelmintic [10], antiproliferative [11], anti-HIV [12], anticonvulsant [13], anti-inflammatory [14], antihypertensive [15], antineoplastic [16] and anti-trichinellosis [17] activities. In addition, they have been used as proteases, since proteases have been linked with several disease states, including thrombosis, inflammation, bronchoconstriction, and tumor growth and invasion [18]. The incorporation of the benzimidazolone nucleus is an important

* Corresponding author.
** Corresponding author. Laboratoire de Chimie Appliquée et Environnement, Equipe de Chimie Bioorganique Appliquée, Faculté des sciences, Université Ibn Zohr, Agadir, Morocco.
E-mail addresses: snounousebbar@gmail.com (N.K. Sebbar), yusufsert1984@gmail.com (Y. Sert).

https://doi.org/10.1016/j.molstruc.2019.127174
0022-2860/

synthetic strategy in studies of antimicrobial drug discovery. Due to the varied bioactivities exhibited by the benzimidazoles, efforts have been made from time to time to generate libraries of these compounds and screen them for potential biological activities [18–23]. They have also been reported to function as precursors for the syntheses of the related compounds, such as *N*-ribosyl-dimethylbenzimidazole present in nature, which serves as an axial ligand for cobalt in vitamin B12 [24], and possesses anti-diabetic [25] and anti-corrosion activities [26–30]. Fig. 1 provides some examples of bioactive molecules possessing benzimidazole moieties [31–33] (see Fig. 2).

In continuation of our research work on the development of *N*-substituted benzimidazole derivatives and evaluation of their potential pharmacological activities recently performed by our team [16,34], it seemed interesting to prepare molecules of original structures incorporated with benzimidazole motifs and evaluate their activities. The synthesized compounds (**2**–**5**) were characterized by single crystal X-ray diffraction and Nuclear Magnetic Resonance (^{1}H and ^{13}C NMR) techniques. The structures were confirmed by predicting the corresponding spectroscopic data and Z-matrix coordinates using DFT calculations at the B3LYP/6-31G(d,p) level of theory and molecular docking studies. The compounds (**2**–**5**) were further identified using Hirshfeld surface analyses, molecular docking studies and DFT calculations. Moreover, the antibacterial activities of the compounds (**2**–**5**) were evaluated against gram-positive and gram-negative bacteria such as *Staphylococcus aureus*, *Escherichia coli*, and *Pseudomonas aeruginosa.*

2. Material and methods

2.1. Spectral data measurements

The spectroscopic characterizations of the synthesized compounds (**2**–**5**) were achieved by recording NMR spectra, which were measured on a Bruker Avance DPX 300 instrument. The chemical shifts (δ) were expressed in ppm down field from TMS [tetramethylsilane, $Si(CH_3)_4$], which has been assigned to a chemical shift of zero, TMS as an internal reference. Thin layer chromatography (TLC) and column chromatography were carried out on silica plates (Merck 60 F254) and silica gel (Merck 60, 230–400 mesh), respectively. Melting points of the compounds (**2**–**5**) were measured in open capillaries and were uncorrected.

2.2. Syntheses of compounds (2–5) by alkylation reactions under PTC conditions

Initially, we prepared benzimidazolone **2** by condensation of *o*-phenylenediamine **1** with ethyl acetoacetate in xylene at reflux for 6 h (**Step a**). Thereafter, 1-(prop-1-en-2-yl)-3-(prop-2-ynyl)-1H-benzimidazol-2(3H)-one **3** was prepared with a good yield (91%) *via* alkylation reaction of compound **2** by propargyl bromide under phase transfer catalysis (PTC) conditions using tetra-*n*-butylammonium bromide (TBAB) as a catalyst and potassium hydroxide as a base in CH_2Cl_2 at room temperature (**Step b**) (Scheme 1). In this paper, we present the synthesis of benzimidazolone **4** by means of N-3 deprotection (**Step c**) as described by Weber et al., 1992 [35] and Mondieig et al., 2013 [19]. The action of benzyl chloride on **4** in hot DMF, for 6 h in the presence of tetra *n*-butylammonium bromide (TBAB) as a catalyst and K_2CO_3 as a base, led to production of alkylated product **5** in good yield (76%) (**Step d**) (Scheme 1). The structures of the compounds (**2**–**5**) were determined by the usual spectroscopic methods, such as ^{1}H NMR, ^{13}C NMR, and were further confirmed by X-ray crystallographic studies.

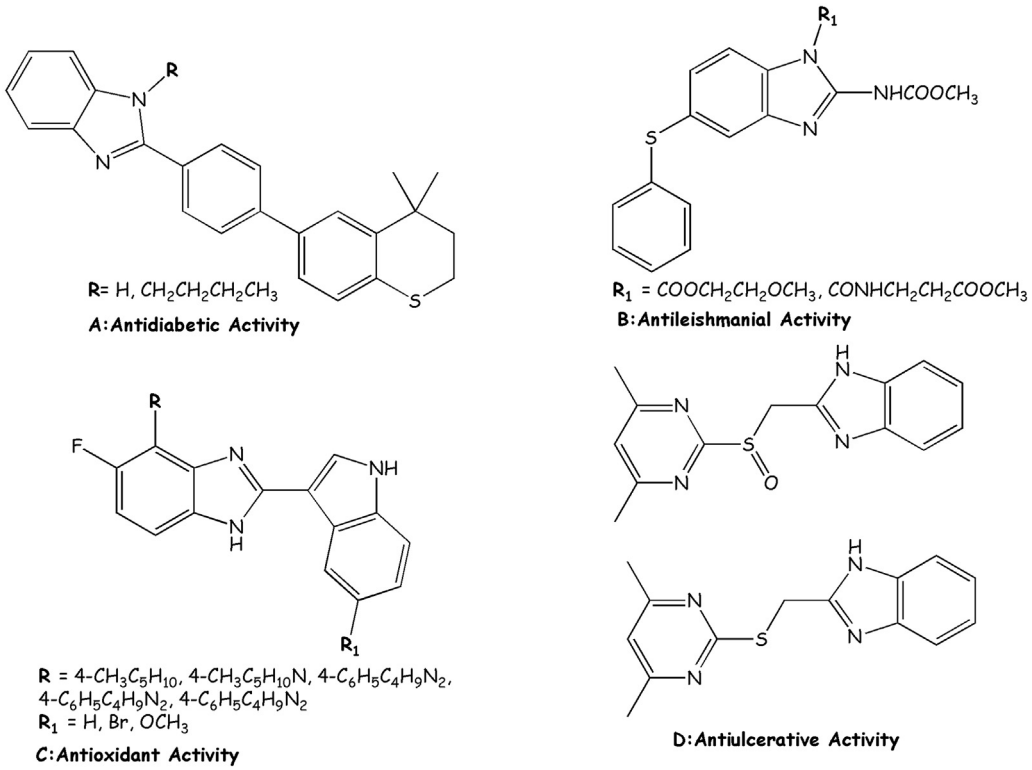

Fig. 1. Examples of bioactive molecules derived from benzimidazoles.

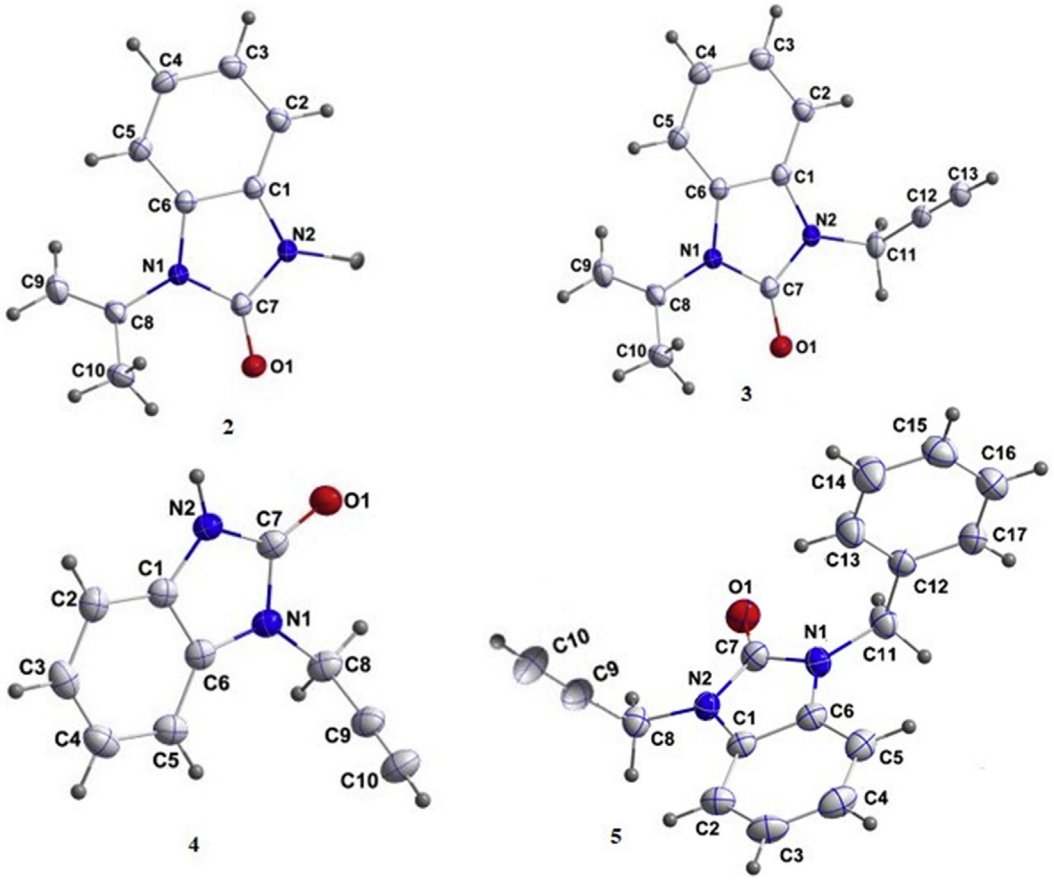

Fig. 2. ORTEP plots with the ellipsoids drawn at the 50% probability level of the compounds (**2**–**5**). **2:** 1-(prop-1-en-2-yl)-1H-benzoimidazol-2(3H)-one: [31]; **3:** 1-(prop-1-en-2-yl)-3-(prop-2-ynyl)-1H-benzoimidazol-2(3H)-one; **4:** 1-(prop-2-ynyl)-1H-benzoimidazol-2(3H)-one and **5:** 1-benzyl-3-(prop-2-yn-1-yl)-2,3-dihydro-1H-1,3-benzodiazol -3-one.

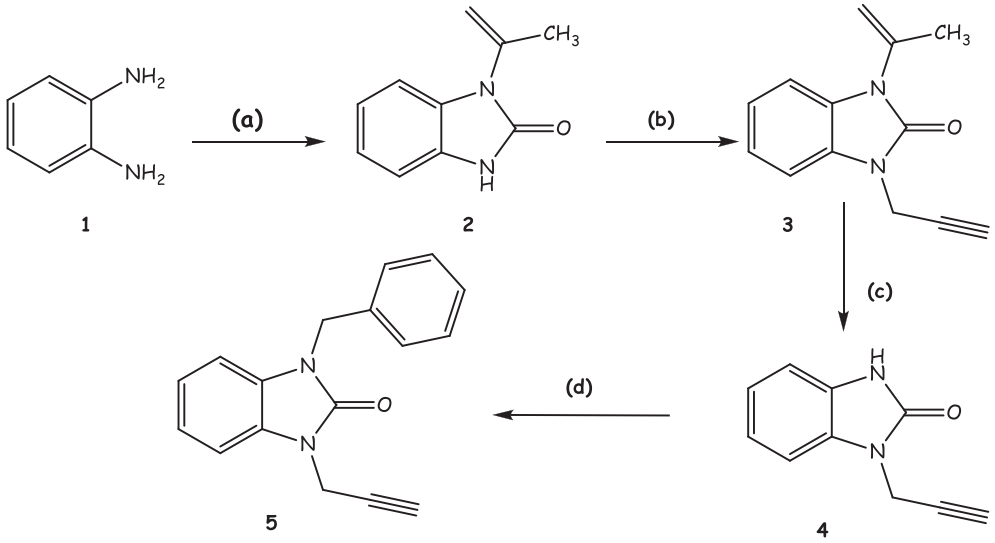

(**a**): Ethyl acetoacetate/xylene/ reflux/ 6 h;
(**b**): $BrCH_2C{\equiv}CH$/ NaOH/ TBAB/ CH_2Cl_2;
(**c**): Cold H_2SO_4 50%, rt, 12 h;
(**d**): $ClCH_2Ph$, DMF, K_2CO_3, TBAB, rt, 24 h.

Scheme 1. Syntheses of benzimidazole derivatives (**2**–**5**).

2.2.1. Experimental part

2.2.1.1. Procedure for the synthesis of 2 [36]. *o*-Phenylenediamine (1.0 g, 9 mmol) and ethyl acetoacetate (1.2 mL, 9 mmol) were heated in xylene (10 mL) for 6 h. The mixture was set aside for the growth of colourless crystals of *N*-isopropenyl benzimidazol-2-one (yield, 90%).

2.2.1.2. 1-Isopropenyl-1H-1,3-benzimidazol-2(3H)-one: 2. Yield (%) = 90%; mp = 392 K; **^{1}H NMR (300 MHz, CDCl$_3$):** 22.24 (d, 3H, $^4J_{H\text{-}H}$ = 3 Hz, CH_3),5.25 (d, 1H, $^4J_{H\text{-}H}$ = 3 Hz, CH_2), 5.40 (d, 1H, $^4J_{H\text{-}H}$ = 3 Hz, CH_2), 7.05−7.14 (m, 4H, CH_{arom}),10.00 (s, 1H, NH). **^{13}C NMR (75 MHz, CDCl$_3$):** 154.44 (C═O), 137.84 (Cq), 130.27 (Cq), 128.27 (Cq), 121.93 (CH_{arom}), 121.43 (CH_{arom}), 113.93 (CH_2), 109.79 (CH_{arom}), 109.14 (CH_{arom}), 20.22 (CH_3).

2.2.1.3. Procedure for the synthesis of 3. Propargyl bromide (11.4 mmol) was added to a mixture of 1-isopropenyl-1H-1,3-benzimidazol-2(3H)-one **2** (5.7 mmol), potassium hydroxide (5.7 mmol) and tetra-*n*-butyl ammonium bromide (0.15 mmol) in CH_2Cl_2 (15 mL). Stirring was continued at room temperature for 48 h. Salts were removed by filtration, and the filtrate was concentrated under reduced pressure. The residue obtained was purified by recrystallization from ethanol to obtain colourless crystals in 91% yield.

2.2.1.4. 1-(Prop-1-en-2-yl)-3-(prop-2-ynyl)-1H-benzimidazol-2(3H)-one: 3. Yield (%) = 91; mp = 331 K; **^{1}H NMR (300 MHz, CDCl$_3$):** 2.22 (d, 3H, $^4J_{H\text{-}H}$ = 3 Hz, CH_3), 2.30 (t, 3H, $^3J_{H\text{-}H}$ = 3 Hz, CH), 4.69 (d, 2H, $^4J_{H\text{-}H}$ = 3 Hz, $\underline{CH_2}C{\equiv}CH$), 5.20 (d, 1H, $^4J_{H\text{-}H}$ = 3 Hz, CH_2), 5.35 (d, 1H, $^4J_{H\text{-}H}$ = 3 Hz, CH_2), 7.10−7.30 (m, 4H, CH_{arom}). **^{13}C NMR (75 MHz, CDCl$_3$):** 151.99 (C═O), 137.99 (Cq), 129.07 (Cq), 128.72 (Cq), 121.86 (CH_{arom}), 121.78 (CH_{arom}), 113.32 (CH_2), 109.20 (CH_{arom}), 108.57 (CH_{arom}), 77.06(CH), 72.82 ($\underline{C}{\equiv}CH$), 30.40 (CH_2), 20.22 (CH_3).

2.2.1.5. Procedure for the synthesis of 4. A solution of 1-(prop-1-en-2-yl)-3-(prop-2-ynyl)-1H-benzoimidazol-2(3H)-one **3** (7.0 mmol) in DMF (10 mL) was treated with a cold sulfuric acid solution (15 mL, 50%) for 12 h. The precipitate obtained was filtered, washed several times with water and subsequently with acetone, and dried to obtain **4,** in 75% yield [34].

2.2.1.6. 1-(Prop-2-ynyl)-1H-benzoimidazol-2(3H)-one, 4. Yield (%) = 75; mp = 399 K; **^{1}H NMR (300 MHz, DMSO):** 3.31 (t, 1H, $^3J_{H\text{-}H}$ = 3 Hz, CH), 4.68 (d, 2H, $^4J_{H\text{-}H}$ = 3 Hz, $\underline{CH_2}C{\equiv}CH$), 7.04−7.21 (m, 4H, CH_{arom}), 10.99 (s, 1H, NH)·**^{13}C NMR (75 MHz, DMSO):**154.01 (C═O), 129.79 (Cq), 128.72 (Cq), 121.86 (CH_{arom}), 121.17 (CH_{arom}), 109.44 (CH_{arom}), 108.75 (CH_{arom}), 79.01 (CH), 74.99 ($\underline{C}{\equiv}CH$), 29.85 (CH_2).

2.2.1.7. Procedure for the synthesis of 5: [37]. To a solution of 1-(prop-2-ynyl)-1H-benzoimidazol-2(3H)-one (3.42 mmol), benzyl chloride (6.81 mmol), and potassium carbonate (6.42 mmol) in DMF (15 mL), a catalytic amount of tetra-*n*-butylammonium bromide (0.37 mmol) was added. The mixture was stirred for 24 h, the solid material was removed by filtration, and the solvent was evaporated under vacuum. The solid product obtained was purified by recrystallization from ethanol to obtain colourless crystals in 76% yield.

2.2.1.8. 1-Benzyl-3-(prop-2-ynyl)-benzimidazol-2-one, 5. Yield (%) = 76; mp = 361 k; **^{1}H NMR (300 MHz, CDCl$_3$):** 2.30 (t, 1H, $^3J_{H\text{-}H}$ = 3 Hz, CH), 4.72 (d, 2H, $^4J_{H\text{-}H}$ = 3 Hz, $\underline{CH_2}C{\equiv}CH$), 5.07 (s, 2H, CH_2), 6.87−7.32 (m, 9H, CH_{arom}). **^{13}C NMR (75 MHz, DMSO):** 153.65 (C═O), 136.17 (Cq), 129.38 (Cq), 128.82 ($2CH_{arom}$), 128.57 (Cq), 127.80 (CH_{arom}), 127.55($2CH_{arom}$), 121.83 (CH_{arom}), 121.58 (CH_{arom}), 108.54 (CH_{arom}), 108.50 (CH_{arom}), 77.16(CH), 72.81 ($\underline{C}{\equiv}CH$), 45.10 (CH_2-Ph), 30.67 (CH_2).

2.3. Single crystal X-ray diffraction

2.3.1. Crystal structures of benzimidazole derivatives (2−5)

The molecular and crystal structures of the benzimidazole derivatives (**2**−**5**), which were obtained by condensation, N-3 deprotection and alkylation reactions were clarified. It is interesting to note that all compounds crystallize in the monoclinic system with the space groups of $P2_1/c$ (for compounds **3**−**5**) and *C 2/c* (for compound **2**). The crystallographic data have been deposited in Cambridge Crystallographic Data Center (CCDC) with the deposition numbers of **CCDC NC2184** (for compound **2**), **CCDC 1941910** (for compound **3**), **CCDC GK2546** (for compound **4**) and **CCDC 1879**758 (for compound **5**).

2.4. Theoretical details

Recently, Density Functional Theory (DFT) method has been demonstrated to have an advantage in computations of organic or inorganic compounds because of its superiority over other methods. This method is very crucial due to both cost of calculations and reliable results for complex molecules in quantum chemistry; the foundation of this method was established in the 1970s. From a literature survey, we can say that the DFT method is used in many fields from dense matter physics and computational physics to computational chemistry and the method is both popular and versatile. In this theorem an "s" function, usually Becke 3-Lee-Yang-Parr (B3LYP) is preferred, which is probably the best one [38,39]. In this study, for computations by the B3LYP and 6-31G(d,p) methods, the basis set was selected and all calculations were carried out employing the Gaussian 09 W package program [40]. Furthermore, the Gauss View 9 interface program [41] was used for visualization of properties of the computed quantities. Firstly, molecular optimizations of the compounds (**2**−**5**) were carried out starting with the atom coordinates determined by the crystallographic studies and other computations were made based on the optimized structures. Calculations of the intermolecular interactions were performed using the Crystal Explorer 3.1 program [42]; this method is known as the Hirshfeld surface analysis. Also, in this study, Highest Occupied Molecular Orbital (HOMO) and Lowest Unoccupied Molecular Orbital (LUMO) analysis of the compounds (**2**−**5**) were performed and the distributions of the groups were obtained using the Chemissian software [43]. Later, ^{1}H and ^{13}CNMR chemical shifts of the compounds (**2**−**5**) were computed by using the GIAO-Gauge-Including Atomic Orbital approach with the B3LYP functional and a 6-31G(d,p) basis set, and then compared with the experimental NMR spectra in a DMSO solution. Finally, molecular docking studies between the compounds (**2**−**5**) and topoisomerase II enzyme (PDB code: 1JIJ) were carried out employing the AutoDockVina free software program [44] (see Table 1).

3. Results and discussion

3.1. Molecular structures

As can be seen in Fig. 3, the compounds (**2**−**5**) are out of plane (all structures have C_1 symmetry) and the atom numbering schemes were those used in the structure determinations. Each compound was optimized starting from the observed crystal

Table 1
Experimental details.

	Compound 2 [36]	Compound 3	Compound 4	Compound 5
Crystal data				
CCDC Deposition number	NC2184	1941910	GK2546	1879758
Chemical formula	$C_{10}H_{10}N_2O$	$C_{13}H_{12}N_2O$	$C_{10}H_8N_2O$	$C_{17}H_{14}N_2O$
Mr	174.20	212.25	172.18	262.30
Crystal system, space group	Monoclinic, C2/c	Monoclinic, P_1c	Monoclinic, $P2_1/c$	Monoclinic, $P2_1/c$
Temperature (K)	100	150	150	298
a, b, c (Å)	15.8724 (2), 6.0971 (1), 17.9313 (3)	15.3197 (4), 9.4602 (2), 7.2933 (2)	4.5116 (2), 17.9709 (7), 10.6508 (4)	8.3567 (2), 9.2040 (2), 17.7868 (4)
β (°)	90.961 (2)	92.467 (1)	94.405 (2)	94.559 (1)
V (Å3)	1735.07 (5)	1056.02 (5)	860.99 (6)	1363.74 (5)
Z	8	4	4	4
Radiation type	Mo K_α	Cu K_α	Cu K_α	Cu K_α
μ (mm−1)	0.09	0.69	0.72	0.64
Crystal size (mm)	0.35 × 0.30 × 0.18	0.28 × 0.12 × 0.05	0.37 × 0.09 × 0.02	0.23 × 0.20 × 0.19
Data collection				
Diffractometer	Bruker X8 APEXII	Bruker D8 VENTURE PHOTON 100 CMOS	Bruker D8 VENTURE PHOTON 100 CMOS	Bruker D8 VENTURE PHOTON 100 CMOS
No. of measured, independent and observed [I > 2σ(I)] reflections	2231	7854, 2053, 1838	6789, 1586, 1319	13551, 2778, 2433
Rint	0.023	0.030	0.053	0.032
Refinement				
R[F2> 2σ(F2)], wR(F2), S	0.039, 0.114, 0.98	0.036, 0.090, 1.05	0.041, 0.100, 1.13	0.038, 0.108, 1.05
No. of reflections	2506	2053	1586	2778
No. of parameters	123	183	150	238
Δρmax, Δρmin (e Å−3)	0.39, 0.21	0.24, −0.25	0.18, −0.22	0.15, −0.12

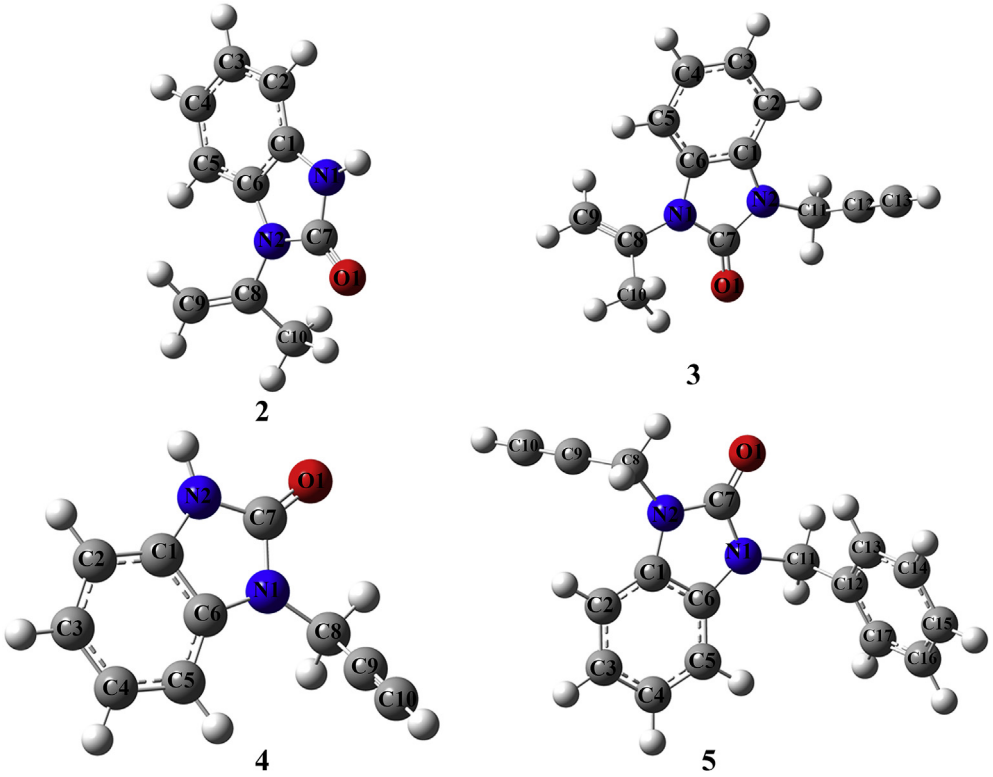

Fig. 3. The optimized structures of benzodiazaol-2-one derivatives (**2**–**5**).

structure using the B3LYP method and 6-31G(d,p) basis set and the bond lengths and angles were determined. Important optimized parameters and their experimental values are given in Table 2. The experimental values were in the solid phase but the calculated values were in the gas phase, so some differences may be seen as frequently occurred.

To the best of our knowledge, no computational analysis of **3** appears in the literature; however, compounds (**2**, **4** and **5**) were examined as previously reported [36,37]. When we focused on the benzimidazol-2-one group, which is common to all structures, the N1–C7, N2–C7, and O1=C7 bond lengths were calculated as 1.390 Å, 1.409 Å and 1.219 Å (for **2**), 1.404 Å, 1.395 Å and 1.221 Å (for

Table 2
The selected optimized structure parameters of the title compounds (2–5).

Bond angles (°)			Bond lenghts (Å)		
Optimized bond angles	X-Ray	DFT/B3LYP/6–31 G(d,p)	Optimized bond lenghts	X-Ray	DFT/B3LYP/6–31 G(d,p)
Compound 2					
C7–N1–C1	110.29 (7)	111.5	O1–C7	1.2338 (11)	1.219
C4–C5–H5	121.5	121.2	C3–H3	0.9500	1.085
C7–N1–H1	122.5 (11)	121.1	N1–C7	1.3663 (11)	1.390
C1–N1–H1	127.2 (11)	127.3	C4–C5	1.3963 (13)	1.400
C5–C6–N2	131.94 (8)	132.1	N1–C1	1.3868 (11)	1.388
O1–C7–N2	125.86 (8)	128.0	C4–H4	0.9500	1.085
O1–C7–N1	127.42 (8)	127.0	N1–H1	0.871 (9)	1.006
C6–N2–C8	126.52 (7)	126.8	C5–C6	1.3827 (12)	1.390
C7–N2–C6	109.21 (7)	106.6	N2–C7	1.3878 (11)	1.409
C9–C8–N2	119.50 (8)	120.1	N2–C6	1.4016 (10)	1.405
N1–C1–C6	107.14 (7)	106.5	C8–C9	1.3225 (14)	1.337
C1–C2–C3	117.45 (9)	117.6	N2–C8	1.4319 (11)	1.430
C4–C3–C2	120.99 (9)	120.9	C8–C10	1.4960 (13)	1.504
N2–C8–C10	115.54 (8)	115.6	C1–C6	1.3999 (11)	1.410
C2–C1–N1	131.46 (8)	131.8			
N1–C7–N2	106.72 (7)	105.0			
C7–N2–C8	124.13 (7)	123.5			
Compound 3					
C7–N1–C6	109.41(10)	109.5	N2–C11	1.4525(16)	1.450
C7–N1–C8	123.86(10)	123.5	O1–C7	1.2233(15)	1.221
C6–N1–C8	126.44(10)	126.9	N1–C7	1.3925(15)	1.404
C7–N2–C1	110.51(10)	110.5	N1–C6	1.4035(16)	1.405
C7–N2–C11	123.10(11)	121.6	N1–C8	1.4301(15)	1.430
C1–N2–C11	126.22(11)	127.7	N2–C7	1.3812(16)	1.395
C2–C1–N2	130.92(11)	131.4	N2–C1	1.3890(16)	1.391
C2–C1–C6	122.11(11)	121.6	C8–C9	1.3280(19)	1.336
N2–C1–C6	106.97(10)	106.9	C8–C10	1.4909(18)	1.504
C5–C6–N1	132.25(11)	132.0	C1–C2	1.3836(18)	1.389
C1–C6–N1	107.05(10)	107.2	C4–C5	1.3942(19)	1.401
O1–C7–N2	126.53(11)	126.2	C5–C6	1.3822(17)	1.389
O1–C7–N1	127.46(11)	128.0	C1–C6	1.3980(17)	1.409
N2–C7–N1	106.01(10)	105.7	C3–C4	1.3933(19)	1.398
C9–C8–N1	119.88(12)	120.1	C2–C3	1.3923(19)	1.400
C9–C8–C10	124.03(12)	124.3			
N1–C8–C10	116.07(11)	115.6			
Compound 4					
C7–N1–C6	109.64(12)	110.6	O1–C7	1.239(2)	1.220
C7–N1–C8	124.23(14)	121.6	N1–C7	1.382(2)	1.400
C6–N1–C8	126.11(13)	127.8	N1–C6	1.395(2)	1.394
C7–N2–C1	110.06(13)	111.3	N1–C8	1.455(2)	1.453
C5–C6–N1	131.43(15)	131.9	N2–C7	1.364(2)	1.391
C1–C6–N1	106.58(13)	106.9	N2–C1	1.390(2)	1.391
C2–C1–N2	131.56(15)	132.3	C1–C2	1.383(2)	1.388
C2–C1–C6	121.25(15)	121.3	C1–C6	1.391(2)	1.411
N2–C1–C6	107.19(13)	106.5	C2–C3	1.388(2)	1.401
O1–C7–N2	127.89(14)	128.1	C2–H5	0.951(19)	1.085
O1–C7–N1	125.60(14)	127.1	C3–C4	1.388(3)	1.397
N2–C7–N1	106.51(14)	104.8	C3–H4	0.97(2)	1.085
N1–C8–C9	111.29(13)	113.8	C4–C5	1.391(3)	1.401
C10–C9–C8	176.99(18)	178.7	C4–H3	0.94(2)	1.085
C9–C10–H10	177.6(15)	179.0	C5–C6	1.384(2)	1.389
C1–C2–C3	116.99(16)	117.6			
C2–C3–C4	121.76(17)	121.2			
Compound 5					
C7–N1–C6	110.18(9)	110.1	O1–C7	1.2163(15)	1.225
C7–N1–C11	123.09(10)	122.2	N1–C7	1.3823(16)	1.392
C6–N1–C11	126.62(10)	127.7	N1–C6	1.3869(15)	1.394
C7–N2–C1	110.34(9)	110.2	N1–C11	1.4632(15)	1.458
C7–N2–C8	123.32(11)	122.0	N2–C7	1.3775(16)	1.396
C1–N2–C8	126.34(11)	128.0	N2–C1	1.3875(15)	1.394
C2–C1–N2	131.74(11)	131.8	N2–C8	1.4525(16)	1.453
C2–C1–C6	121.46(11)	121.4	C1–C2	1.3737(17)	1.388
N2–C1–C6	106.80(10)	106.8	C1–C6	1.3985(16)	1.411
O1–C7–N2	126.95(12)	127.0	C2–C3	1.383(2)	1.401
O1–C7–N1	127.23(12)	127.3	C2–H2	0.959(17)	1.084
N2–C7–N1	105.82(10)	105.8	C3–C4	1.384(2)	1.398
N2–C8–C9	111.93(11)	113.8	C4–C5	1.388(2)	1.401
N1–C11–C12	113.05(10)	114.0	C9–C10	1.166(2)	1.207
C5–C6–N1	132.12(11)	131.8			
C2–C3–C4	121.16(13)	121.2			
C3–C4–C5	121.56(14)	121.3			

3), 1.400 Å, 1.391 Å and 1.220 Å (for **4**) and 1.392 Å, 1.396 Å and 1.225 Å (for **5**), respectively, using the B3LYP method and 6-31G(d,p) basis set.

Regarding 1-[(1-benzyl-1H-1,2,3-triazol-4-yl)methyl]-6-methoxy-1H-benzimidazol-2(3H)-one [45], the N1−C1, N2−C1, and O1−C1 (according to the given atom numbering scheme) the bond lengths were calculated as 1.359 Å, 1.383 Å and 1.242 Å, respectively, using the DFT/B3LYP method/function. In this study, the basis set, D95V++**, by El Bakri et al. [45] was used.

In the present study, the N1−C7−O1, N2−C7−O1 and N1−C7−N2 bond angles were computed as 127.0°, 128.0° and 105.0° (for **2**), 128.0°, 126.2° and 105.7° (for **3**), 127.1°, 128.1° and 104.8° (for **4**) and 127.3°, 127.0° and 105.8° (for **5**), respectively, employing the DFT/B3LYP method and 6-31G(d,p) basis set. For 1-[(1-benzyl-1H-1,2,3-triazol-4-yl)methyl]-6-methoxy-1H-benzimidazol-2(3H)-one [45], the N1−C1−O1, N2−C1−O1 and N1−C1−N2 bond angles were calculated as 127.82°, 125.65° and 106.53°, respectively, using the DFT/B3LYP method and D95V++** basis set level. Furthermore, comparison of the selected theoretical bond lengths and angles by the B3LYP method and 6-31G(d,p) basis set show that there is an excellent agreement between them. The other optimized molecular structure parameters can be seen and compared in Table 2.

3.2. Hirshfeld surface calculations

The Hirshfeld surface analyses of the compounds (**2**–**5**) were carried out by using Crystal Explorer 3.1 program [41]. In these calculations, the experimental atom positions were used to obtain the intermolecular contacts and the contributions of the inter-contacts related to the Hirshfeld surfaces, which are presented in Fig. 4(a–d) and Figs. S1–S3 (Supporting Information a-d since Hirshfeld surface analyses have been reported previously for the compounds **2**, **4** and 5). For **3**, Fig. 4 (a) represents the 3D Hirshfeld surface (D_{norm}), and Fig. 4(b–d) represent the 2D fingerprint plots. In the figures, the three colours are represented on the surfaces; red, blue and white. The dark red spots indicate powerful hydrogen bond points in the crystals, white spots indicate contacts near the van der Waals separation, and blue spots indicate longer contacts [46–49]. As can be seen in Fig. 4 (a), the interacting distances for O−H, H−H, and C−H bonds were obtained as 2.326 Å, 2.525 Å to 2.863 Å, and 2.958 Å to 3.659 Å, respectively. Finally, the contributions of the inter-contacts to the Hirshfeld surfaces are H−H (52.2%), C−H/H−C (23.8%) and O−H/H−O (11%); the quantitative results of the Hirshfeld surface analysis are shown in Fig. 4(b–d).

3.3. HOMO-LUMO analyses

Considering the fact that HOMO-LUMO energies are the key factors in defining quantum chemical interactions, the importance of this analysis becomes clearer [50]. The highest occupied molecular orbital (HOMO) energies, the lowest unoccupied molecular orbital (LUMO) energies, and their related quantities and orbital distributions (percentage distribution according to the related groups) of the compounds (**2**–**5**) were computed using the DFT/B3LYP method and 6-31G(d,p) basis set. The contributions to HOMOs and LUMOs, and HOMO and LUMO energy values and other related parameters of the compounds (**2**–**5**) are tabulated in Tables 3 and 4, respectively, and the resulting orbital pictures are shown in Fig. 5. In Table 3, the contributions to HOMOs and LUMOs are determined by employing the Chemissian software [43] as shown. As can be seen, the group with the highest electron density is the benzimidazol-2-one moiety for both HOMO and LUMO distributions, that is, both HOMOs and LUMOs are mainly concentrated in this group. This indicates that the electronic transitions and charge transfers are over this group. Additionally, the HOMO–LUMO gaps of the compounds (**2**–**5**) were calculated as 5.401 eV, 5.426 eV, 5.500 eV and 5.381 eV, respectively. From these results, we can conclude that the sum of the electronic and zero-point energies of compound **5** is relatively low (the most stable structure according to the energy results) and its gap is small. Furthermore, by using HOMO and LUMO values, other crucial parameters such as the ionization potential, electron affinity, chemical hardness, electronic chemical potential, electrophilicity index and

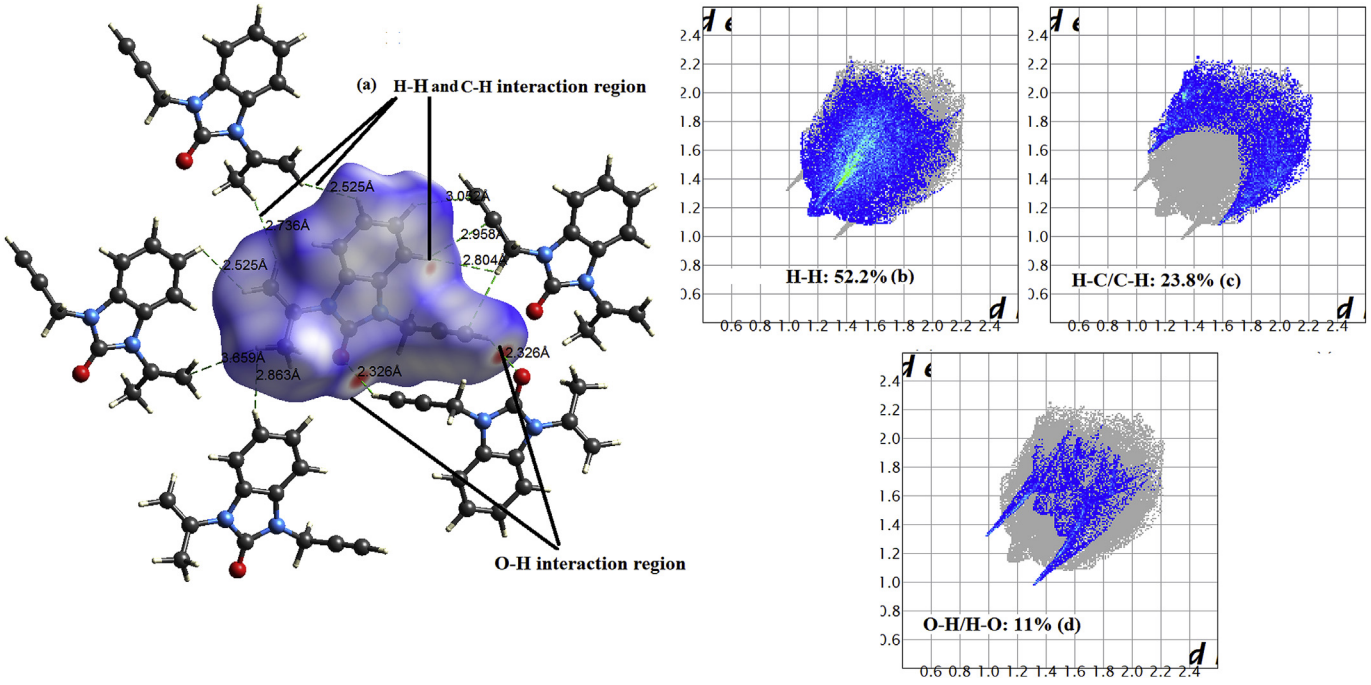

Fig. 4. The 3D Hirshfeld surface (a) and 2D fingerprint histograms of **3**.

Table 3
The contributions to HOMOs and LUMOs of compounds (2–5).

MOs	**Compound 2**		
	Benzoimidazol-2-one	Prop-1-en-2yl	
HOMO	93%	7%	
LUMO	89%	11%	
MOs	**Compound 3**		
	Benzoimidazol-2-one	Prop-1-en-2yl	Prop-2-ynyl
HOMO	93%	6%	1%
LUMO	86%	14%	0%
MOs	**Compound 4**		
	Benzoimidazol-2-one	Prop-2-ynyl	
HOMO	98%	2%	
LUMO	100%	0%	
MOs	**Compound 5**		
	Benzoimidazol-2-one	Prop-2-ynyl	benzyl
HOMO	95%	1%	4%
LUMO	11%	0%	89%

softness were also calculated (Table 3).

3.4. NMR analyses

The theoretical ^{1}H NMR and ^{13}C NMR chemical shifts were calculated using $CDCl_3$ solutions (for **2**, **3** and **5)** and DMSO-d_6 (for **4)** by the DFT/B3LYP and 6-31G(d,p) basis set method with the application of IEFPCM model and GIAO method. The experimental and calculated proton ^{1}H and ^{13}C NMR chemical shifts are shown in Tables 5 and 6.

3.5. Molecular docking studies

For understanding the binding interactions between a ligand and its receptor, molecular docking studies are very important especially for drug design. In this section, molecular docking analyses were performed with the help of the AutoDockVina program [44]. In the computations, both the ligands and receptor pdb (protein data bank) formats were prepared using the Discover Studio Visualizer 4.0 (DSV 4.0) software [51] and pdb format for the target receptor was obtained from the Protein Data Bank [52,53]. For the analysis between the ligands (**2**–**5**) and topoisomerase II enzyme**-**1 JIJ (receptor), the molecular docking positions (grid positions) were taken as $38 \times 58 \times 124$ Å^3, $40 \times 40 \times 126$ Å^3, $40 \times 40 \times 126$ Å^3 and $44 \times 52 \times 126$ Å^3, respectively. According to the rotatable bonds of the ligands (**2**–**5**), ten modes were superposed and their affinity energy values and root mean square (RMS) values were calculated (Table 7). From Table 7, we can surmise that the best docking pose is between **4** and 1JIJ receptor with a binding energy of −6.6 kcal/mol involving two hydrogen bonds. Additionally, the inhibition constant (K_i) is 14.5266×10^{-6} M (for **4**) derived from $K_i = \exp(\Delta G/RT)$, where ΔG, R and T are the binding free energy, gas constant (1.9872036×10^{-3} kcal/mol) and room temperature (298.15 K), respectively. This docking model is shown in Fig. 6 (a and b). Most of the hydrogen bonding interactions (Fig. 6) is between the GLU302 residue and H1 with a bond distance of 2.94 Å and between LYS305 residue and O1 atom with a 3.09 Å distance, additionally, there are π-π stacking interactions between the PHE273-PHE306 residues and the centroid of the benzimidazole

Table 4
HOMO and LUMO Energy Values and other related parameters of compounds (2–5).

Parameters (eV)	Compound 2	Compound 3	Compound 4	Compound 5
E_{LUMO} (eV)	−0.221	−0.200	−0.177	−0.212
E_{HOMO} (eV)	−5.622	−5.627	−5.677	−5.593
Energy band gap $\lvert E_{HOMO}\text{-}E_{LUMO}\rvert$	5.401	5.426	5.500	5.381
Ionization potential ($I = -E_{HOMO}$)	5.622	5.627	5.677	5.593
Electron affinity ($A = -E_{LUMO}$)	0.221	0.200	0.177	0.212
Chemical hardness ($h = (I\text{-}A)/2$)	2.700	2.713	2.750	2.690
Chemical softness ($z = 1/2h$)	0.185	0.184	0.182	0.186
Electronegativity ($\chi = (I + A)/2$)	2.922	2.914	2.927	2.903
Chemical potential ($\mu = -(I + A)/2$)	−2.922	−2.914	−2.927	−2.903
Electrophilicity index ($w = \mu^2/2h$)	1.581	1.564	1.558	1.566
Sum of Electronic and zero-point Energies (a.u)	−571.661776	−687.073056	−570.418136	−840.681218

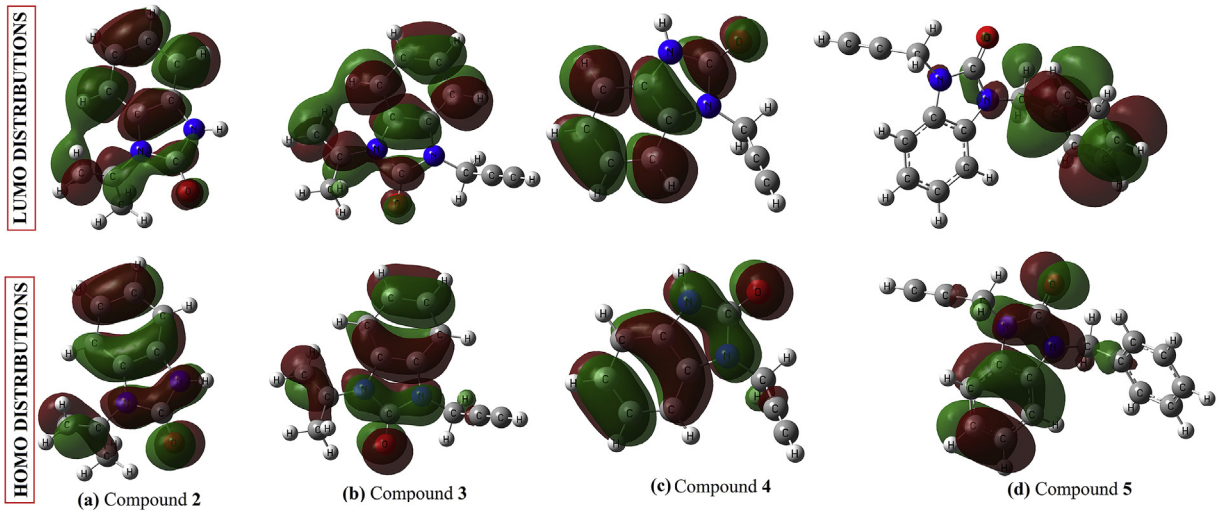

Fig. 5. HOMO and LUMO plots of **2**–**5** in B3LYP/6-31G(d,p).

Table 5
The experimental and computed[13]C NMR isotropic chemical shifts (with respect to TMS, all values are in ppm) of compounds (2–5).

2			3			4			5		
Atoms	$\delta_{exp.}$	$\delta_{cal.}$	Atoms	$\delta_{exp.}$	$\delta_{cal.}$	Atoms	$\delta_{exp.}$	$\delta_{cal.}$	Atoms	$\delta_{exp.}$	$\delta_{cal.}$
C1	128.27	116.29	C1	129.07	117.54	C1	128.72	115.88	C1	129.38	116.96
C2	109.79	97.21	C2	108.57	97.64	C2	109.44	97.85	C2	108.54	97.39
C3	121.93	109.99	C3	121.86	110.16	C3	121.86	110.31	C3	121.58	109.75
C4	121.43	109.49	C4	121.78	110.04	C4	121.17	109.88	C4	121.83	109.98
C5	109.14	98.02	C5	109.20	98.02	C5	108.75	97.53	C5	108.50	97.02
C6	130.27	118.67	C6	128.72	117.62	C6	129.79	117.87	C6	136.17	117.73
C7	154.44	136.89	C7	151.99	137.06	C7	154.01	137.47	C7	153.65	139.22
C8	137.84	131.62	C8	137.99	131.62	C8	29.85	24.01	C8	30.67	24.57
C9	113.93	99.61	C9	113.32	100.08	C9	74.99	64.45	C9	72.81	64.16
C10	20.22	13.24	C10	20.22	13.28	C10	79.01	60.00	C10	77.16	60.13
			C11	30.40	24.10				C11	45.10	39.62
			C12	72.82	63.98				C12	128.57	126.92
			C13	77.06	60.15				C13	128.82	116.99
									C14	128.82	117.01
									C15	127.80	115.66
									C16	127.55	115.90
									C17	127.55	116.55

Table 6
The experimental and computed [1]H NMR isotropic chemical shifts (with respect to TMS, all values are in ppm) of compounds (2–5).

2			3			4			5		
Atoms	$\delta_{exp.}$	$\delta_{cal.}$	Atoms	$\delta_{exp.}$	$\delta_{cal.}$	Atoms	$\delta_{exp.}$	$\delta_{cal.}$	Atoms	$\delta_{exp.}$	$\delta_{cal.}$
H1		6.75	H2	7.10–7.30	7.55	H1		7.00	H2	6.87–7.32	7.51
H2	7.05–7.14	7.23	H3		7.49	H5	7.04–7.21	7.55	H3		7.43
H3		7.39	H4		7.48	H4		7.51	H4		7.39
H4		7.41	H5		7.49	H3		7.51	H5		7.34
H5		7.45	H9A	5.35	5.72	H2		7.38	H8A	4.72	4.42
H9A	5.25	5.48	H9B	5.20	5.48	H8A	4.68	4.42	H8B	4.72	5.45
H9B	5.40	5.68	H10A	2.22	2.05	H8B	4.68	5.24	H10	2.30	2.23
H10A	2.24	2.00	H10B	2.22	2.02	H10	3.31	2.29	H11A	5.07	4.41
H10B	2.24	3.59	H10C	2.22	3.59	NH2	10.99		H11B	5.07	5.81
H10C	2.24	1.98	H11A	4.69	4.37				H13	6.87–7.32	8.03
NH1	10.0		H11B	4.69	5.36				H14		7.72
			H13	2.30	2.23				H15		7.65
									H16		7.71
									H17		7.82

Table 7
AutoDockVina results of the binding affinity and RMSD values of different poses in 1JIJ inhibitor of compounds 2–5.

Mode	2-1JIJ			3-1JIJ		
	Affinity (kcal/mol)	rmsdl.b.	rmsdu.b.	Affinity (kcal/mol)	rmsdl.b.	rmsdu.b.
1	−6.5	0.000	0.000	−5.9	0.000	0.000
2	−5.6	20.458	21.739	−5.8	36.198	37.853
3	−5.3	36.621	37.555	−5.6	36.572	38.498
4	−5.3	20.140	21.310	−5.6	37.662	39.435
5	−5.3	1.731	2.873	−5.5	35.963	37.762
6	−5.3	10.553	12.161	−5.4	19.720	21.405
7	−5.2	20.467	21.663	−5.4	11.303	13.549
8	−5.1	20.070	21.413	−5.1	36.933	38.758
9	−5.1	40.735	41.840	−5.0	36.729	38.493
10	−5.0	2.531	3.338	−4.9	1.528	3.927
Mode	4-1JIJ			5-1JIJ		
	Affinity (kcal/mol)	rmsdl.b.	rmsdu.b.	Affinity (kcal/mol)	rmsdl.b.	rmsdu.b.
1	−6.6	0.000	0.000	−6.5	0.000	0.000
2	−6.2	23.334	24.717	−6.4	3.613	5.677
3	−5.4	1.816	2.125	−5.4	41.713	43.692
4	−5.4	20.775	22.032	−5.4	2.130	3.961
5	−5.4	20.805	22.065	−5.2	2.707	5.852
6	−5.3	37.308	38.393	−5.1	23.257	24.770
7	−5.2	30.494	31.430	−5.1	21.777	23.109
8	−5.2	19.363	20.805	−5.0	23.218	25.255
9	−5.1	20.042	21.409	−4.9	23.357	25.933
10	−5.0	21.277	22.643	−4.8	12.323	15.645

unit. For ligands (**2**, **3** and **5**), the molecular docking surfaces around the ligands and 2D structures are given in Figs. S4–S6 (Supporting Information).

Finally, the molecular docking results revealed that ligands (**2**, **3** and **5**) may exhibit some activities against the active site of topoisomerase II enzyme; from this point of view, this study will be useful to take a step forward for future antibacterial studies.

4. Study of antibacterial activity

4.1. Microorganism used and inoculum preparation

The microorganisms tested included the following bacteria: *Staphylococcus aureus* (*ATCC-25923*), *Escherichia coli* (*ATTC-25922*), and *Pseudomonas aeruginosa* (*ATCC-27853*). All pathogenic microorganisms isolated from patients were stored in the culture collection of the Microbiology Department (Microthec Unity) at the National Institute of Hygiene (Rabat, Morocco). They were maintained in a brain heart infusion (BHI) at −80 °C. Prior to the experiment, the cultures were prepared by sub-culturing 1 mL of each culture stock in 9 mL of BHI broth.

4.2. Disc diffusion method

The "agar disc diffusion method" was employed for the determination of the antibacterial activities of the synthesized compounds (**2**–**5**). The principle of this technique is to estimate the bacteriostatic activities of the antibacterial agents by measuring the growth inhibition zones of the bacteria around the discs impregnated with the test samples placed on the agar plates. It is mostly used as a preliminary step to further studies, because it provides access to essential qualitative results. We have adapted a similar method described in some studies [54,55]. The test samples were firstly dissolved in DMSO (1%), which does not have an adverse effect on microbial growth. Briefly, the test was performed in sterile petri plates containing an agar medium. Sterile medium (30 mL) was poured into petri plates, and after solidification, 100 µL [10^6 colony-forming units (cfu)/mL] of fresh cultures of different bacterial species (one microorganism per petri plate) were swabbed on the plates. Sterile filter paper discs (6 mm in diameter), impregnated with 6 µL of each sample at a concentration of 50 mg/mL, were placed on the surface of the agar. The petri plates were sealed with sterile laboratory film to avoid evaporation of the test samples, and then incubated at 30 °C for 24 h. Diameters of the inhibition zones were measured in millimetres (mm). In addition, the antibacterial activities of the synthesized compounds (**2**–**5**) were compared with commercially available antibiotics, such as chloramphenicol (Chlor) and ampicillin (Amp). 1% DMSO alone was used as a negative control. The plates were then incubated at 37 °C for 24 h. After incubation, the diameter of the zones of inhibition were measured in mm and recorded [56,57]. The experiment was carried out in triplicate. Compounds (**2**–**5**) showed an average antibacterial activity (Fig. 7 and Table 8).

The results are presented in the form of antibiograms below:

Disc diffusion assays were employed to determine the MIC of the compounds (**2**–**5**). The results of the antibacterial activity of the compounds (**2**–**5**) exhibit growth inhibition in the three bacterial strains (*Staphylococcus aureus*, *Escherichia coli*, and *Pseudomonas aeruginosa*). Compound **2** obtained by the condensation of *o*-phenylenediamine **1** with ethyl acetoacetate gave an anti-bacterial activity of **MIC** = 12.5 µg/mL for *Staphylococcus aureus*, *Pseudomonas aeruginosa*, and **MIC** = 3.125 µg/mL for *Escherichia coli*. Moreover, in order to increase the inhibitory activity of **2** we alkylated it with propargyl bromide. Interestingly, the presence of a prop-1-yne group in compounds (**3**, **4,** and **5**) showed a similar activity against the two bacterial strains as that tested by **5**, with an **MIC** of 12.5 µg/mL for *Escherichia coli* and *Pseudomonas aeruginosa* and **MIC** = 3.125 µg/mL for *Staphylococcus aureus*. However, compound **3** showed a better activity with an MIC of 6.25 µg/mL for *Staphylococcus aureus*, 25 µg/mL for *Pseudomonas aeruginosa*, and 12.5 µg/mL for *Escherichia coli*. Indeed, the deprotection of N-3 of compound **3** also showed a better activity, with an MIC of 12.5 µg/mL for *Staphylococcus aureus* and *Escherichia coli*, and 25 µg/mL for *Pseudomonas aeruginosa*. Notably that the derivatives functionalized with ester groups and benzene rings possess the highest antibacterial activity (92% of the pathogenic bacteria were sensitive to these compounds). Studies, such as, anti-inflammatory, antifungal, antiparasitic, and anti-cancer tests should also be performed, as the literature reveals a lot of interesting results on these subjects. Also, other bacteria should be tested to expand this investigation.

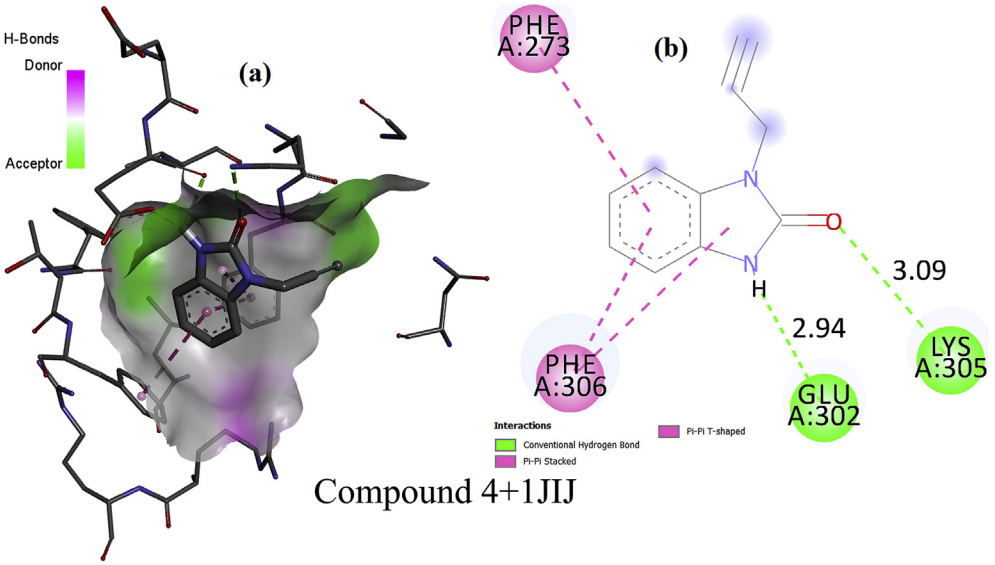

Fig. 6. The molecular docking results of **4** with 1JIJ protein, surfaces around ligand (a) and 2D forms (b).

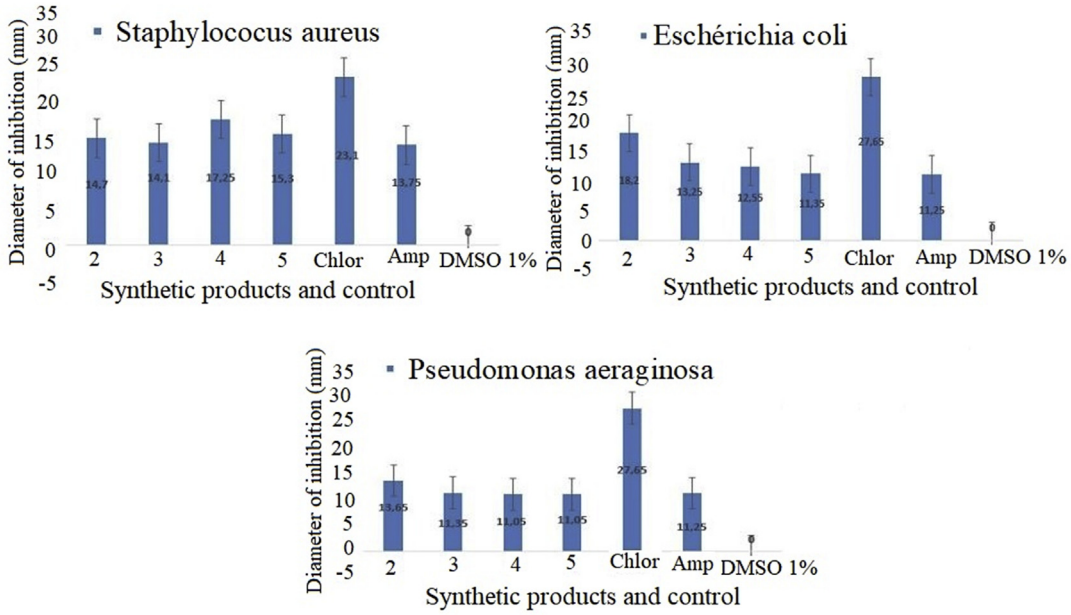

Fig. 7. Antibacterial activities of the compounds (**2**–**5**) vis-a-vis bacteria tested (*Staphylococcus aureus, Escherichia* coli and *Pseudomonas aeruginosa*) are summarized in the figure below. Chlor, Chloramphenicol (30 μg/mL); Amp, Ampicillin (10 μg/mL); DMSO, dimethylsulfoxyde (1%).

Table 8
Antibacterial activity of the compounds (2–5) represented as Minimum Inhibitory Concentration [MIC (μg/mL)].

Compounds	MIC (μg/mL)			
	Staphylococcus aureus	*Escherichia coli*	*Pseudomonas aeruginosa*	*Staphylococcus aureus*
2	12.5	3.125	12.5	12.5
3	6.25	12.5	25	6.25
4	3.125	6.25	6.25	3.125
5	6.25	12.5	12.5	6.25
Chlor	12.5	6.25	6.25	12.5

5. Conclusions

The studies performed in this work show that benzimidazole constitutes an interesting core present in several drugs and natural products Moreover, we report the synthesis of novel benzimidazole derivatives **2**–**5**. Their structures have been elucidated thanks to X-ray crystallography and spectroscopic techniques. The theoretical approach used allows a relatively good reproduction of X-ray geometrical parameters, spectral data, and ^{1}H and ^{13}C NMR chemical shifts. Hirshfeld surface analysis was employed to confirm the existence of intermolecular interactions in compounds **2**–**5**. The experimental spectroscopic data were well reproduced by using quantum chemical DFT and in silico based molecular docking studies. The benzimidazolone derivatives **2**–**5** exhibited antibacterial activity and could act as potent antibacterial compounds.

Acknowledgements

The authors extend their appreciation to the Deanship of Scientific Research at King Saud University for participating in this work through research group no (RG- 1440-141). Authors would like to thank Prof. Dr. Fatih Ucun for his helpful contribution and Gaussian Calculations and JTM thanks Tulane University for support of the Tulane Crystallography Laboratory.

Appendix A. Supplementary data

Supplementary data to this article can be found online at https://doi.org/10.1016/j.molstruc.2019.127174.

Abbreviations

Chlor	Chloramphenicol
Amp	Ampicillin
DMSO	dimethylsulfoxyde
MIC	Minimum Inhibitor Concentration
BHI	Brain heart infusion
HOMO	highest occupied molecular orbital
LUMO	lowest unoccupied molecular orbital
DSV 4.0	Discover Studio Visualizer 4.0

References

[1] Y. Özkay, Y. Tunalı, H. Karaca, İ. Işıkdağ, Antimicrobial activity and a SAR study of some novel benzimidazole derivatives bearing hydrazone moiety, Eur. J. Med. Chem. 45 (8) (2010) 3293–3298.
[2] S. Kumar, R. Saini, H. Singh, Silver selective benzimidazol-2 (1H)-one based, sulphur-containing podands, J. Inclusion Phenom. Mol. Recognit. Chem. 11 (2) (1991) 115–119.
[3] S.-P. Olesen, E. Munch, P. Moldt, J. Drejer, Selective activation of Ca2+-dependent K+ channels by novel benzimidazolone, Eur. J. Pharmacol. 251 (1) (1994) 53–59.
[4] G.S. Baxter, D.E. Clarke, Benzimidazolone derivatives act as 5-HT4 receptor ligands in rat oesophagus, Eur. J. Pharmacol. 212 (2–3) (1992) 225–229.
[5] G. Rémond, B. Portevin, J. Bonnet, E. Canet, D. Regoli, G. De Nanteuil,

Pharmacological profile of a novel series of NK1 antagonists. In vitro and in vivo potency of benzimidazolone derivatives, Eur. J. Med. Chem. 32 (11) (1997) 843–868.
[6] L. Al-Nakkash, S. Hu, M. Li, T.-C. Hwang, A common mechanism for cystic fibrosis transmembrane conductance regulator protein activation by genistein and benzimidazolone analogs, J. Pharmacol. Exp. Ther. 296 (2) (2001) 464–472.
[7] A. Cuthbert, M. Hickman, P. Thorn, L. MacVinish, Activation of Ca2+-and cAMP-sensitive K+ channels in murine colonic epithelia by 1-ethyl-2-benzimidazolone, Am. J. Physiol. Cell Physiol. 277 (1) (1999) C111–C120.
[8] M. Gaba, S. Singh, C. Mohan, Benzimidazole: an emerging scaffold for analgesic and anti-inflammatory agents, Eur. J. Med. Chem. 76 (2014) 494–505.
[9] G. Ayhan-Kılcıgil, C. Kus, E.D. Özdamar, B. Can-Eke, M. Iscan, Synthesis and antioxidant capacities of some new benzimidazole derivatives, Arch. Pharm.: Int. J. Pharm. Med. Chem. 340 (11) (2007) 607–611.
[10] G. Navarrete-Vázquez, R. Cedillo, A. Hernández-Campos, L. Yépez, F. Hernández-Luis, J. Valdez, R. Morales, R. Cortés, M. Hernández, R. Castillo, Synthesis and antiparasitic activity of 2-(trifluoromethyl) benzimidazole derivatives, Bioorg. Med. Chem. Lett 11 (2) (2001) 187–190.
[11] E. Ravina, R. Sanchez-Alonso, J. Fueyo, M. Baltar, J. Bos, R. Iglesias, M. Sanmartin, Antiparasitic activity of some New Caledonian medicinal plants, Arzneim. Forsch. 43 (1993) 684–694.
[12] L. Garuti, M. Roberti, M. Malagoli, T. Rossi, M. Castelli, Synthesis and antiproliferative activity of some benzimidazole-4, 7-dione derivatives, Bioorg. Med. Chem. Lett 10 (19) (2000) 2193–2195.
[13] A. Rao, A. Chimirri, E. De Clercq, A.M. Monforte, P. Monforte, C. Pannecouque, M. Zappalà, Synthesis and anti-HIV activity of 1-(2, 6-difluorophenyl)-1H, 3H-thiazolo [3, 4-a] benzimidazole structurally-related 1, 2-substituted benzimidazoles, Il Farmaco 57 (10) (2002) 819–823.
[14] P.A. Thakurdesai, S.G. Wadodkar, C.T. Chopade, Synthesis and anti-inflammatory activity of some benzimidazole-2-carboxylic acids, Pharmacologyonline 1 (2007) 314–329.
[15] B. Serafin, G. Borkowska, J. Główczyk, I. Kowalska, S. Rump, Potential antihypertensive benzimidazole derivatives, Pol. J. Pharmacol. Pharm. 41 (1) (1989) 89–96.
[16] A.-h. Abdel-monem, New synthesis and antineoplastic activity of substituted 3, 4-dihydro-and 1, 2, 3, 4-tetrahydro-benzo [4, 5] imidazo [1, 2-a] pyrinnidine derivatives, Arch Pharm. Res. (Seoul) 30 (2007) 78–684.
[17] A.T. Mavrova, P. Denkova, Y.A. Tsenov, K.K. Anichina, D.I. Vutchev, Synthesis and antitrichinellosis activity of some bis (benzimidazol-2-yl) amines, Bioorg. Med. Chem. 15 (18) (2007) 6291–6297.
[18] J. Béahdy, Recent developments of antibiotic research and classification of antibiotics according to chemical structure. Advances in applied microbiology, Elsevier, 1974, pp. 309–406.
[19] D. Mondieig, L. Lakhrissi, A. El Assyry, B. Lakhrissi, P. Negrier, E.M. Essassi, M. Massoui, J.M. Leger, B. Benali, Synthesis and structural study of some bis-benzimidazol-2-one derivatives by x-ray diffraction, Moroccan J. Heterocyclic Chem. 12(1) 51-61.
[20] B. Lakhrissi, A. Benksim, M. Massoui, E.M. Essassi, V. Lequart, N. Joly, D. Beaupère, A. Wadouachi, P. Martin, Towards the synthesis of new benzimidazolone derivatives with surfactant properties, Carbohydr. Res. 343 (3) (2008) 421–433.
[21] Y. Ouzidan, Y. Kandri Rodi, F.R. Fronczek, R. Venkatraman, L. El Ammari, E.M. Essassi, 1, 3-Bis [2-(2-oxo-1, 3-oxazolidin-3-yl) ethyl]-1H-benzimidazol-2 (3H)-one, Acta Crystallogr. E: Struct. Rep. Online 67 (2) (2011) o362–o363.
[22] A. Saber, N.K. Sebbar, T. Hökelek, B. Hni, J.T. Mague, E.M. Essassi, Crystal structure and Hirshfeld surface analysis of 1-{[2-oxo-3-(prop 1-en-2-yl)-2, 3-dihydro-1H-1, 3-benzodiazol-1-yl] methyl}-3-(prop-1-en-2-yl)-2, 3-dihydro-1H-1, 3-benzodiazol-2-one, Acta Crystallogr. E: Crystallogr. Commun. 74 (12) (2018) 1746–1750.
[23] D. Mondieig, P. Negrier, J.-M. Léger, L. Lakhrissi, A. El Assyry, B. Lakhrissi, E.M. Essassi, B. Benali, A. Boucetta, Synthesis and structural study of N-isopropenylbenzimidazolone, Russ. J. Phys. Chem. 89 (5) (2015) 807–811.
[24] R. Walia, M. Hedaitullah, S.F. Naaz, K. Iqbal, H. Lamba, Benzimidazole derivatives–an overview, IJRPC 1 (3) (2011) 565–574.
[25] B. Kumar, P. Rao, Synthesis and structural studies on transition metal complexes derived from 1-(2-thienyl)-1-ethanole-1H-benzimidazole, Asian J. Chem. 18 (2006) 3060–3064.
[26] T. Yanardag, S. Dinçer, A. Aksüt, Corrosion inhibition efficiency of benzimidazole and benzimidazole derivatives for zinc, copper and brass, Asian J. Chem. 24 (1) (2012) 47–52.
[27] X. Wang, Y. Wan, Y. Zeng, Y. Gu, Investigation of benzimidazole compound as a novel corrosion inhibitor for mild steel in hydrochloric acid solution, Int. J. Electrochem. Sci 7 (2012) 2403–2415.
[28] Y. Abboud, B. Hammouti, A. Abourriche, B. Ihssane, A. Bennamara, M. Charrouf, S. Al-Deyab, 2-(O-Hydroxyphenyl) benzimidazole as a new corrosion inhibitor for mild steel in hydrochloric acid solution, Int. J. Electrochem. Sci 7 (2012) 2543–2551.
[29] M. Benabdellah, A. Tounsi, K. Khaled, B. Hammouti, Thermodynamic, chemical and electrochemical investigations of 2-mercapto benzimidazole as corrosion inhibitor for mild steel in hydrochloric acid solutions, Arabian J. Chem. 4 (1) (2011) 17–24.
[30] H. Shukla, G. Udayabhanu, M. Mirdha, S. Mondal, Synergistic corrosion inhibition of mild steel by some Mercaptobenzidazol compounds with halide ions in sulfuric acid solution 56, 2013, pp. 13363–13369.
[31] J. Shukla, S. SAXENA, R. RASTOGI, Synthesis OF some newer. 1-HETEROCYCLIC AMINO/IMINOMETHYL-2-SUBSTITUTED benzimidazoles as a potent CNS; anticonvulsant and MONOAMINEOXIDASE inhibitory agents, Curr. Sci. (1982) 820–822.
[32] Z. Ateş-Alagöz, C. Kuş, T. Çoban, Synthesis and antioxidant properties of novel benzimidazoles containing substituted indole or 1, 1, 4, 4-tetramethyl-1, 2, 3, 4-tetrahydro-naphthalene fragments, J. Enzym. Inhib. Med. Chem. 20 (4) (2005) 325–331.
[33] J. Bariwal, A. Shah, M. Kathiravan, R. Somani, J. Jagtap, K. Jain, Synthesis and antiulcer activity of novel pyrimidylthiomethyl-and pyrimidylsulfinylmethyl benzimidazoles as potential reversible proton pump inhibitors, Indian J. Pharm. Ed. Res. 42 (3) (2008) 225–231.
[34] A. Saber, N.K. Sebbar, T. Hökelek, Y. Ouzidan, Y.K. Rodi, M. Elhafi, J.T. Mague, E.M. EssassI, Crystal structure and hirshfeld surface analysis of 1-(prop-2-yn-1-yl)-2,3-dihydro-1H-1,3-benzodiazo-2-one, Moroccan J. Heterocyclic Chem. 17 (2) (2018) 92–101.
[35] E. Weber, M. Piel, H.J. Buschmann, E. Cleve, Synthese und Komplexbildung eines neuen makrocyclischen Liganden mit drei Benzimidazolin-2-on-Einheiten, Chem. Ber. 125 (11) (1992) 2483–2485.
[36] A. Saber, H. Zouihri, E.M. Essassi, S.W. Ng, 1-Isopropenyl-1H-1, 3-benzimidazol-2 (3H)-one, Acta Crystallogr. E: Struct. Rep. Online 66 (6) (2010) o1409-o1409.
[37] A. Saber, N.K. Sebbar, T. Hökelek, J. Mague, E. Essassi, Crystal structure and Hirshfeld surface analysis of 1-benzyl-3-(prop-2-yn-1-yl)-2, 3-dihydro-1H-1, 3-benzodiazol-2-one, Acta Crystallogr. E: Crystallogr. Commun. 74 (12) (2018) 1842–1846.
[38] A.D. Becke, Density-functional thermochemistry. I. The effect of the exchange-only gradient correction, J. Chem. Phys. 96 (3) (1992) 2155–2160.
[39] R.G. Parr, Density Functional Theory of Atoms and Molecules, Horizons of Quantum Chemistry, Springer, 1980, pp. 5–15.
[40] M.J. Frisch, G. Trucks, H. Schlegel, G. Scuseria, M. Robb, J. Cheeseman, G. Scalmani, V. Barone, B. Mennucci, G. Petersson, Gaussian 09, Revision D. 01, Gaussian, Inc., Wallingford, CT, 2009.
[41] R. Dennington, T. Keith, J. Millam, GaussView, Version 5, Semichem Inc., Shawnee Mission, KS, 2009.
[42] M. Turner, J. McKinnon, S. Wolff, D. Grimwood, P. Spackman, D. Jayatilaka, M. Spackman, CrystalExplorer. Version 17, University of Western Australia, 2017.
[43] S. Leonid, Chemissian software 2017. www.chemissian.com.
[44] O. Trott, A.J. Olson, AutoDock Vina, Improving the speed and accuracy of docking with a new scoring function, efficient optimization, and multithreading, J. Comput. Chem. 31 (2) (2010) 455–461.
[45] Y. El Bakri, C.-H. Lai, J. Sebhaoui, A.B. Ali, Y. Ramli, E.M. Essassi, J.T. Mague, Synthesis, crystal structure, Hirshfeld surface analysis, and DFT calculations of new 1-[(1-benzyl-1H-1, 2, 3-triazol-4-yl) methyl]-6-methoxy-1H-benzimidazol-2 (3H)-one, Chem. Data Collect. 17 (2018) 472–482.
[46] Y.F. Baba, Y. Sert, Y.K. Rodi, S. Hayani, J.T. Mague, D. Prim, J. Marrot, F.O. Chahdi, N.K. Sebbar, E.M. Essassi, Synthesis, crystal structure, spectroscopic characterization, Hirshfeld surface analysis, molecular docking studies and DFT calculations, and antioxidant activity of 2-oxo-1, 2-dihydroquinoline-4-carboxylate derivatives, J. Mol. Struct. 1188 (2019) 255–268.
[47] F.L. Hirshfeld, Bonded-atom fragments for describing molecular charge densities, Theor. Chim. Acta 44 (2) (1977) 129–138.
[48] J.J. McKinnon, M.A. Spackman, A.S. Mitchell, Novel tools for visualizing and exploring intermolecular interactions in molecular crystals, Acta Crystallogr. Sect. B Struct. Sci. 60 (6) (2004) 627–668.
[49] M.A. Spackman, P.G. Byrom, A novel definition of a molecule in a crystal, Chem. Phys. Lett. 267 (3–4) (1997) 215–220.
[50] Z. Zhou, R.G. Parr, Activation hardness: new index for describing the orientation of electrophilic aromatic substitution, J. Am. Chem. Soc. 112 (15) (1990) 5720–5724.
[51] https://www.3dsbiovia.com/.
[52] X. Qiu, C.A. Janson, W.W. Smith, S.M. Green, P. McDevitt, K. Johanson, P. Carter, M. Hibbs, C. Lewis, A. Chalker, Crystal structure of Staphylococcus aureus tyrosyl-tRNA synthetase in complex with a class of potent and specific inhibitors, Protein Sci. 10 (10) (2001) 2008–2016.
[53] RCSB. https://www.rcsb.org/.
[54] J. Sirot, Bactériologie Médicale, Flammarion, Paris, France, 1990.
[55] L. Prescott, J. Harley, D. Klein, Microbiology, 2nd. Edition, vol. 912, Wm C. Brown Communication, Inc., USA, 1993, pp. 325–343.
[56] S.M. Finegold, W.J. Martin, Diagnostic Microbiology, Diagnostic Microbiology, CV Mosby, 1982.
[57] D. Alderman, P. Smith, Development of draft protocols of standard reference methods for antimicrobial agent susceptibility testing of bacteria associated with fish diseases, Aquaculture 196 (3–4) (2001) 211–243.